

Numerical Investigation of Conjugate Natural Convection Heat Transfer from Discrete Heat Sources in Rectangular Enclosure

F. A. Gdhaidh, K. Hussain, and H. S. Qi

Abstract— The coupling between natural convection and conduction within rectangular enclosure was investigated numerically. Three separate heat sources flush mounted on a vertical wall and an isoflux condition was applied at the back of heat sources. Continuity, momentum and energy conservation equations were solved by using control volume formulation and the coupling of velocity and pressure was treated by using the “SIMPLE” algorithm. The modified Rayleigh number and the substrate/fluid thermal conductivity ratio were used in the range $R_{al_z}^* = 10^4 - 10^7$ and $R_s = 10 - 1000$ respectively. The investigation was extended to compare results of FC-77 with Air and also for high values of $R_s > 1000$. The results illustrated that, when the modified Rayleigh number increases, dimensionless heat flux and local Nusselt number increases for both fluids. Opposite behaviour for the thermal spreading in the substrate and the dimensionless temperature θ , they were decreased when $R_{al_z}^*$ is increased. Also with increasing the substrate/fluid thermal conductivity ratio for a given value of the modified Rayleigh number the thermal spreading in the substrate increased which is the reason of the decrease in the maximum temperature value. The present study concluded that, for high values of $R_s > 1500$, the effect of the substrate is negligible.

Keywords— Natural convection, modified Rayleigh number, thermal conductivity ratio, control volume.

I. INTRODUCTION

Coupling between natural convection and conduction heat transfer is evident in many practical applications. In natural convection the fluid movement is created by the buoyancy force due to the temperature difference. Therefore no external force is needed such as fans or coolers which could be the main cause of noise and vibration. Also the conducting solid wall gives additional heat transfer from the heat source to the fluid. The main drawback of natural convection is the rate of heat transfer is small compared to forced convection. Previous researches showed, this problem could be overcome by immersing the system in dielectric liquid [1].

Mr. Farog A. Gdhaidh is PhD student in Faculty of Engineering and Informatics at Bradford University, BD7 1DP, UK (e-mail: F.A.Gdhaidh@bradford.ac.uk)

Dr. Khalid Hussain is Senior Lecturer in Mechanical Engineering and the Head of the School of Engineering at Bradford University, BD7 1DP, UK (e-mail: K.Hussain1@bradford.ac.uk)

Dr. Hong-Sheng Qi is Senior Lecturer in Mechanical Engineering at Bradford University, BD7 1DP, UK and Committee Member of WCE (e-mail: H.Qi@bradford.ac.uk)

Zinnes [2] was the first investigator who studied the conjugate effects in natural convection. He observed that, the coupling between conduction in a substrate and convection in a fluid is hugely affected by the substrate/fluid thermal conductivity ratio.

Most of the published works in the field of natural convection from rectangular enclosures [3-5] whether these enclosures considered vertical or horizontal revealed that, the isothermal condition was applied to create the temperature gradient. Several numerical investigations [6-7] considered the conjugate natural convection from a heater mounted on a substrate immersed in liquid within an enclosure. It was concluded that most of the generated power was dissipated by the substrate for high value of fluid/substrate thermal conductivity ratio and the maximum temperature of the heater decreased. Heindel et al. [8] carried out three dimensional numerical and experimental studies for heat sources mounted on one vertical wall of the cavity and the opposite wall at constant room temperature. The study performed using different coolant fluids (water and FC-77). Their results show that, increasing the modified Rayleigh number, the convection coefficients along the heater face and vertical velocity were also increased. Numerical predictions of steady state natural convection in a square cavity was given by Banerjee et al. [9] to determine the sizes of heaters and the value of applied heat fluxes to ensure the operation within the specified thermal limit. Wroblewski and Joshi [10-11] noticed that, at high substrate/fluid thermal conductivity ratio when $R_s > 10$, the effects of the substrate conductive especially on the maximum temperature were found to be very important due to the low thermal conductivity of the coolant liquid which was used (FC-75). Experimental and numerical studies of conjugate heat transfer on a heated vertical wall were studied by Bilgen [12]. It was noticed that the Nusselt number depends on the Rayleigh number and wall thickness but it is a weak function of conductivity ratio. The thermal performance of the enclosure is improved with an increase in the Rayleigh number as it is noticed by [13-14].

From previous studies, many efforts have been spent for both numerical and experimental methods to investigate the effects of Rayleigh number R_a , substrate/fluid thermal conductivity ratio R_s and different fluids on the flow and temperature fields. It was shown that the maximum temperature is decreased with increasing R_s especially when $R_s > 10$. In the present study the numerical investigation has been used to show that, although the maximum temperature is reduced by increasing R_s , but there is a limit on R_s where the maximum temperature remains constant with increasing R_s over that limit.

II. PROBLEM DESCRIPTION

A numerical investigation of the coupling between conduction and natural convection heat transfer from three discrete heat sources mounted on vertical wall of a cavity has been investigated. The opposite vertical wall and the horizontal walls are assumed to be at constant temperature (isothermal) and adiabatic respectively. Figure 1 show Schematic of the two-dimensional rectangular cavity filled with different fluids FC-77 (a dielectric fluorocarbon liquid) and air individually. The isoflux condition is applied at the back of each heat source whereas the back of the substrate is adiabatic.

The height and length of the cavity are H and $(L_s + L_f)$ respectively. Aspect ratio of the cavity is fixed for all cases with $(A_z = H/L_f = 8)$. Table I illustrates the dimension of the parameters in mm .

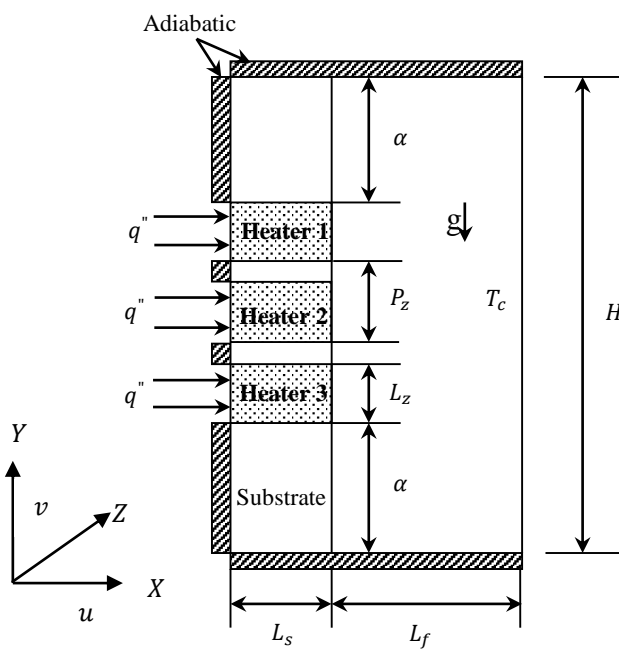


Fig. 1. Schematic diagram of the physical model

Table I. Physical Model Parameters

H	L_z	P_z	L_f	L_s	α
96	12	16.8	12	6	25.2

III. MATHEMATICAL MODEL

The mathematical model is constrained by the following assumptions: 2-D steady state heat transfer, laminar natural convection flow without viscous dissipation, contact resistance between the heater/substrate interfaces and the radiation effects are neglected, the Boussinesq approximation is applied and the gravity acts in the vertical downward direction.

By using the above assumptions in the differential equations of continuity, momentum and energy, the governing equations could be written for both solid and fluid regions in dimensionless form as:

- *Fluid region:*

Continuity:

$$\frac{\partial U}{\partial X} + \frac{\partial V}{\partial Y} = 0 \quad (1)$$

X-momentum:

$$U \frac{\partial U}{\partial X} + V \frac{\partial U}{\partial Y} = -\frac{\partial P}{\partial X} + P_r \left[\frac{\partial^2 U}{\partial X^2} + \frac{\partial^2 U}{\partial Y^2} \right] \quad (2)$$

Y-momentum:

$$U \left[\frac{\partial V}{\partial X} \right] + V \left[\frac{\partial V}{\partial Y} \right] = -\left[\frac{\partial P}{\partial Y} \right] + P_r \left[\frac{\partial^2 V}{\partial X^2} + \frac{\partial^2 V}{\partial Y^2} \right] + R_{al_z}^* P_r \quad (3)$$

Energy:

$$U \frac{\partial \theta}{\partial X} + V \frac{\partial \theta}{\partial Y} = \frac{\partial^2 \theta}{\partial X^2} + \frac{\partial^2 \theta}{\partial Y^2} \quad (4)$$

- *Solid region:*

In this region there is only energy equation because the velocity components are zero.

$$K_1 \frac{\partial^2 \theta}{\partial X^2} + K_2 \frac{\partial^2 \theta}{\partial Y^2} = 0 \quad (5)$$

Where K_1 and K_2 could take the values of R_h or R_s depends on the position of the calculation whether in heater or in substrate region and:

$$R_s = \frac{k_s}{k_f}, \quad R_h = \frac{k_h}{k_f}$$

The above equations were obtained using the following dimensionless parameters:

$$X = \frac{x}{L_z}, \quad Y = \frac{y}{L_z}, \quad U = \frac{uL_z}{\alpha_f}, \quad V = \frac{vL_z}{\alpha_f} \quad (6)$$

$$P = \frac{p}{\rho(\alpha_f/L_z)^2}, \quad \theta = \frac{T-T_c}{(q''L_z/k_f)} \quad (7)$$

$$R_{al_z}^* = \frac{g\beta q''L_z^4}{k_f\alpha_f\nu}, \quad P_r = \frac{\nu}{\alpha_f} \quad (8)$$

In order to complete the mathematical model, the following dimensionless boundary conditions were used:

- At $X = 0$,
 $U = V = 0, \partial\theta/\partial X = \begin{cases} -1/R_h & \text{at heater} \\ 0 & \text{at substrate} \end{cases}$

- At $X = (L_s + L_f)/L_z$,

$$U = V = 0, \quad \theta = 0$$

- At $Y = 0$,

$$U = V = 0, \quad \frac{\partial \theta}{\partial Y} = 0$$

- At $Y = H / L_z$,

$$U = V = 0, \quad \frac{\partial \theta}{\partial Y} = 0$$

The local heat transfer coefficient at solid/fluid interface could be defined as $h_s = q'' / (T_{s(x)} - T_c)$ where $T_{s(x)}$ is the local temperature on the surface [9]. Therefore the rate of convection heat transfer at any point in the solid/fluid interface wall could be introduced by the dimensionless number (local Nusselt number $Nu(X)$) based on the length of the heat source and can be written as:

$$Nu(X) = -\frac{K_1}{\theta_w} \left(\frac{\partial \theta}{\partial X} \right)_w \quad (9)$$

IV. SOLUTION PROCEDURE AND VALIDATION

Present study is based on the control volume technique to discretise the governing equations (1-5) and then the resulting algebraic equations are sequentially solved by “TDMA” (Tri-Diagonal Matrix Algorithm). The “SIMPLE” algorithm (semi-implicit method for pressure linked equations) is used to handle the coupling between pressure and velocity which was described by Patankar [15]. To avoid the divergence in the iteration process, Under-relaxation techniques are used to slow down the change from iteration to iteration.

It is noted that, although the solid and fluid regions have different equations, the numerical solutions within the computational domain for continuity, momentum and energy equations are obtained simultaneously in both regions.

The effects of the number of grid size ($Nx * Ny$) has been analysed when the enclosure filled with FC-77. A three different uniform grid size are tested in both directions. The result of dimensionless temperature at solid/fluid interface shows that, a mesh size of $36 * 80$ is used which gives an optimum computational time compare to others and also gives accurate results.

The code is validated against the benchmark results of Heindel et al. [17] who used “SIMPLER” algorithm for coupling of pressure and velocity. In this study “SIMPLE” algorithm is applied. The validation illustrated that, dimensionless temperatures at solid/fluid interface have the same trends and the deviation between them decreased with increase R_{alz}^* . The biggest deviation was at the base of the enclosure with 11% when $R_{alz}^* = 10^4$ and the percentage is reduced to 6% at the top of the enclosure.

V. RESULTS AND DISCUSSION

The geometry analysed is represented in Figure 1. Firstly the numerical study examined the effects of modified Rayleigh number which is based on the applied isoflux condition in the range $R_{alz}^* = 10^4 - 10^7$ for both fluids (FC-77 and air) and then the effect of thermal conductivity ratio R_s examined in the range 10 – 1000 for FC-77 only. The results are obtained at $R_s = 10$ for modified Rayleigh number effects whereas the effect of substrate/fluid thermal conductivity ratio is considered for $R_{alz}^* = 10^6$.

The results obtained in this study are based on an isothermal boundary condition. However in real applications to keep a wall at low constant temperature is unrealistic.

A. Effects of Modified Rayleigh number

Modified Rayleigh number is varied by changing the applied power to each heat source. The heaters material is corresponding to silicon with thermal conductivity ($k_h = 148 W/mK$) producing constant heat flux and the heater/fluid thermal conductivity ratio is $R_h = 2350$ for FC-77 and $R_h = 5627$ for air. Moreover the fluid Prandtl number was assumed to be 25 corresponding to FC-77 and 0.7 to air.

The dimensionless temperatures (θ) at solid/fluid interface for both fluids are displayed in Fig. 2. Results show that, the value of (θ) increases from the cavity base ($y/L_z = 0$) until the leading edge of the heater number three ($y/L_z = 2.1$). The three heaters are recognized by the isothermal lines where each heater has different value. Because of a decline in convection coefficient and rise in the local bulk fluid temperature, the value of θ increases from heater three to reach the maximum value at heater one. At the end of heater one ($y/L_z = 5.9$), the thermal boundary layer disperses and θ goes down moderately with Y .

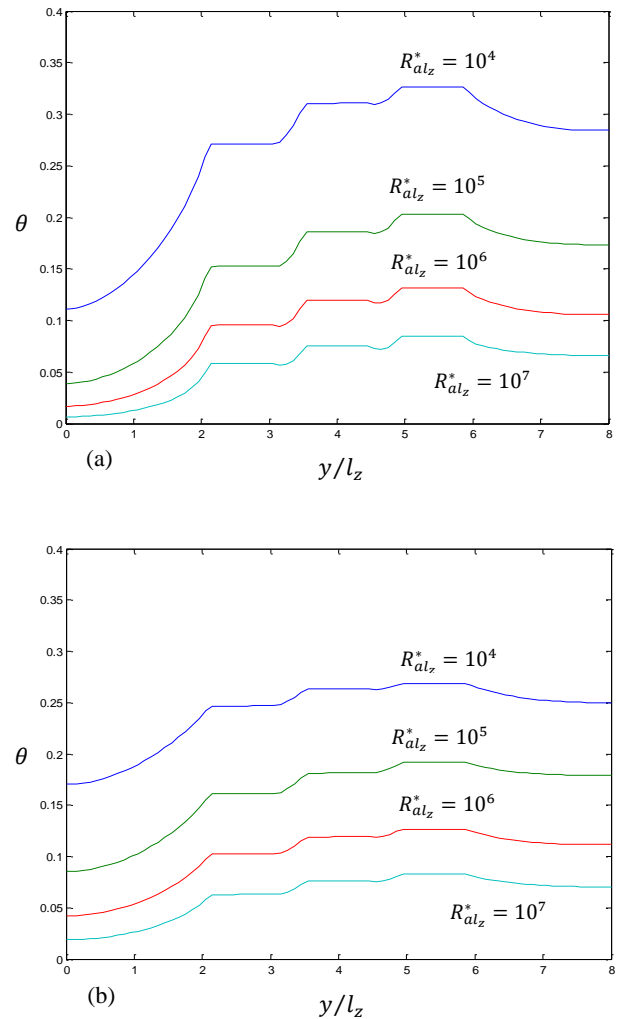


Fig. 2. The local dimensionless temperature profile at the solid/fluid interface for (a) FC-77 $P_r = 25$, $R_h = 2350$ and $R_s = 10$ (b) air $P_r = 0.7$, $R_h = 5627$ and $R_s = 24$.

Further the dimensionless temperature at substrate for air is higher than that of FC-77 while it is lower at heaters for the full range of $R_{al_z}^*$. That because the value of R_s for air is higher than FC-77 where more energy passes to the substrate.

It is evident that, the dimensionless temperature θ decreases as the Rayleigh number $R_{al_z}^*$ increase, this is due to the increase in $(T - T_c)$ is not corresponding to the increase in q'' .

A dimensionless local heat flux could be defined as:

$$\hat{q}'' = q''|_i/q'' \quad (10)$$

where $q''|_i$ is the local interfacial heat flux.

Fig. 3 shows the distribution of \hat{q}'' at solid/fluid interface for both fluids FC-77 and Air respectively. The local peak of heat flux exists at every leading edge of the heater for all cases and that refer to the large temperature differences between the edge and the fluid and also for the high local convection coefficient.

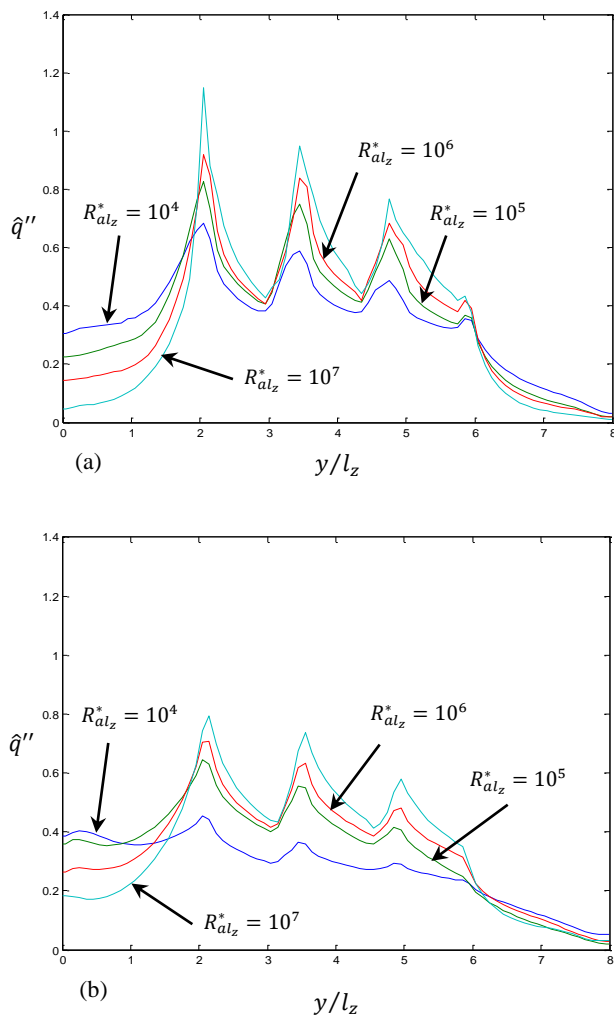


Fig. 3. The local dimensionless heat flux at the solid/fluid interface for (a) FC-77 $P_r = 25$, $R_h = 2350$ and $R_s = 10$ (b) air $P_r = 0.7$, $R_h = 5627$ and $R_s = 24$.

The biggest value of \hat{q}'' is at the leading edge of heater three ($y/L_z = 2.1$) and this value reduced consecutively for heater two and one. It is evident from the figure that, the value of \hat{q}'' increased with increasing $R_{al_z}^*$ because of the

increase thermal boundary layer and decrease the local convection coefficient.

Fig. 3 shows that at a distance ($y/L_z = 5.9$) there is small protrusion for the full range of $R_{al_z}^*$ and that is relative to advection (streamwise conduction) in the fluid. For air the existing of protrusion is masked by the low value of thermal conductivity. In general the advection increases with increasing $R_{al_z}^*$ but convection coefficient increases also and that is the main reason to diminish the effect of streamwise conduction. In comparison between both fluids, increasing R_s to 24 for air increases the thermal spreading within the substrate which is the cause of increasing the values of \hat{q}'' with an associated decrease in \hat{q}'' at the heater locations.

The local Nusselt number $Nu(X)$ variation at solid/fluid interface vertical wall is illustrated in Fig. 4 for the full range of the modified Rayleigh number at a given value of thermal conductivity ratio $R_s = 10$ and $R_s = 24$ for FC-77 and air respectively.

The results indicate that, the local Nusselt number increases with the increase of the Rayleigh number due to the increment in the heat flux which is applied to heaters. As a result the strengthening of buoyancy driven flow increases.

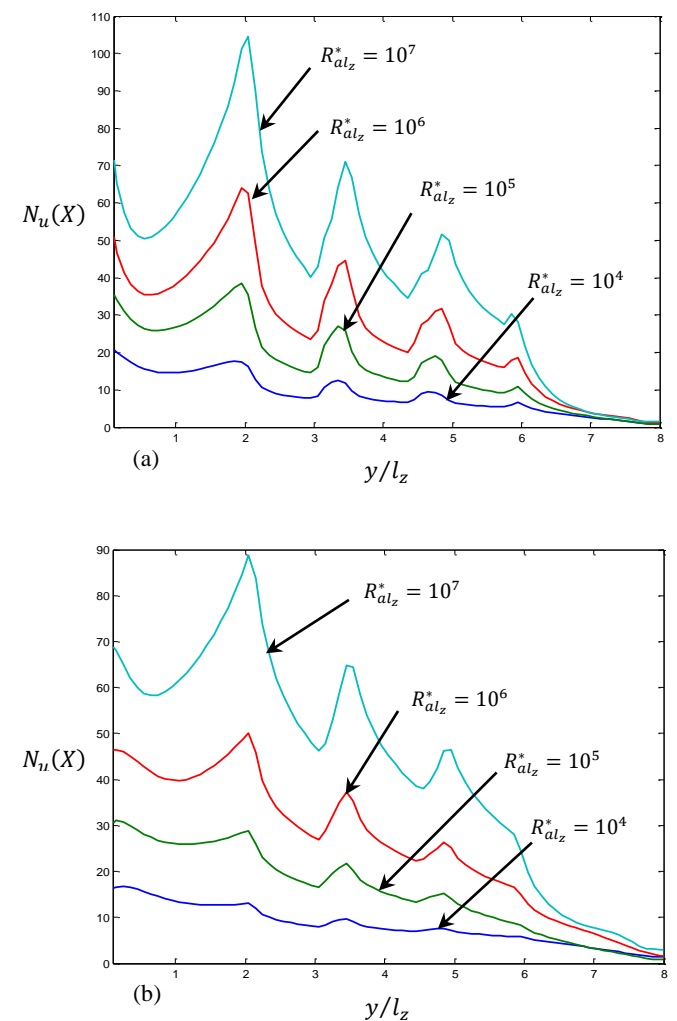


Fig. 4. Local Nusselt number variation at the solid/fluid interface for (a) FC-77 $P_r = 25$, $R_h = 2350$ and $R_s = 10$ (b) air $P_r = 0.7$, $R_h = 5627$ and $R_s = 24$.

Thus the local Nusselt number decreases from the base to the top of the cavity due to the increase in the bulk fluid temperature. The values of local Nusselt number for FC-77 are bigger than that of air because the local convection coefficient of FC-77 is higher than air.

B. Effects of substrate/fluid thermal conductivity ratio

Further investigation has been carried out only for FC-77 with the modified Rayleigh number fixed at $R_{alz}^* = 10^6$. The dimensionless temperature distribution at solid/fluid interface for different values of R_s is shown in Fig. 5. The variations of θ along solid/fluid interface between heater to heater is clearly observed as well as between substrate and heater regions. Increase R_s gives another path to dissipate the heat from heaters where more energy passes through the substrate. If the results between two values $R_s = 10$ and $R_s = 10^3$ are compared, there is a big difference between them at the substrate region under heater three where the dimensionless temperature of $R_s = 10^3$ is about 6 times higher than $R_s = 10$ at the base of the cavity and this difference decreased as y/L_z increase until ($y/L_z = 3.5$) where the values of θ for $R_s = 10$ passed those of $R_s = 10^3$ and the maximum temperature is reduced by 23%. Furthermore the dimensionless temperature over the entire cavity height becomes nearly isothermal for large values of R_s .

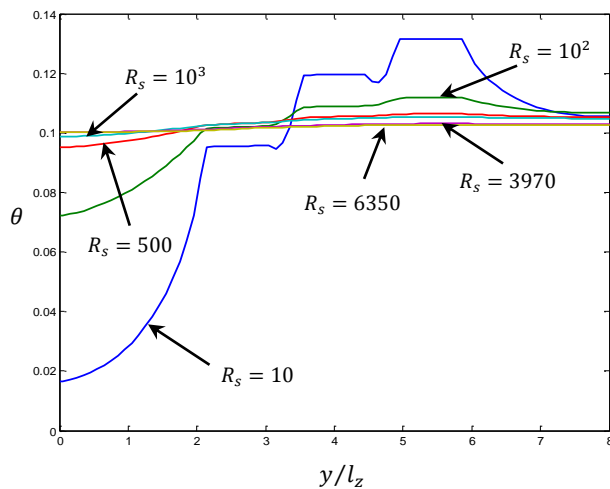


Fig. 5. Local dimensionless temperature distribution at the solid/fluid interface for FC-77 ($P_r = 25, R_h = 2350$ and $R_{alz}^* = 10^6$)

In real applications, copper and aluminium are the preferred materials for the substrate. These two materials have a large thermal conductivity where the thermal conductivity ratios are 6350 and 3970 for copper and aluminium respectively. The results of θ along the solid/fluid interface are converged for both materials, and also the heaters and substrate regions could not be distinguished as shown in Fig. 5. Therefore with very high values of R_s , the effect of thermal conductivity ratio on the dimensionless temperature is disappeared. As a result, the aluminium could be used instead of copper.

C. Temperature results in dimensional form

The previous results are presented in dimensionless form but it is important to know the value of the temperature in dimensional form. From Fig. 6 two values of modified Rayleigh number has been selected $R_{alz}^* = 10^4$ and $R_{alz}^* = 10^5$ for a given value of $R_s = 10$ and $R_s = 24$ for FC-77 and air respectively to present the temperature distribution at solid/fluid interface in dimensional form ($^{\circ}\text{C}$).

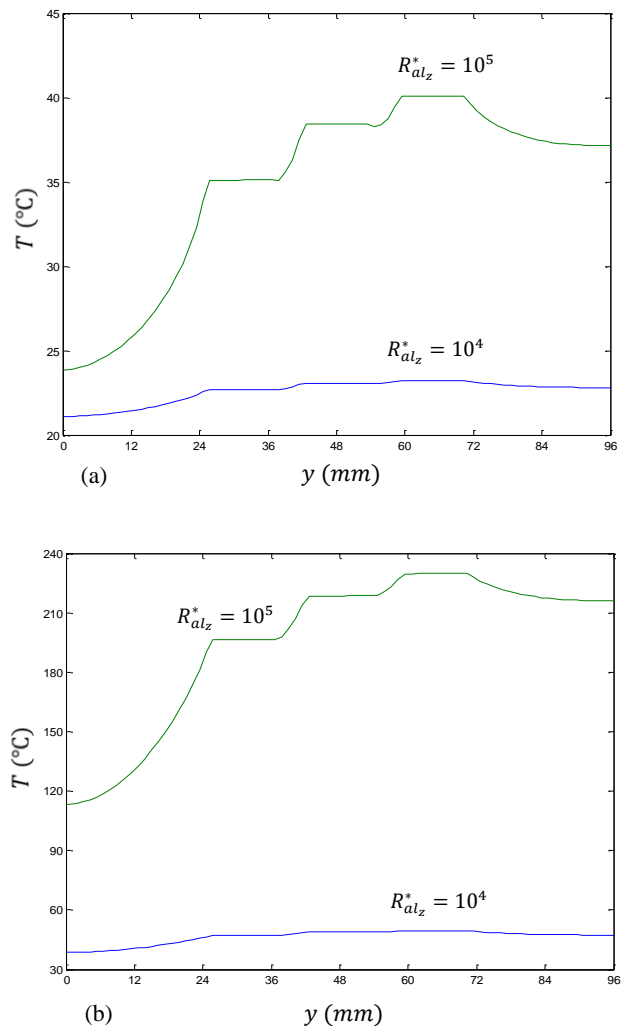


Fig. 6. Local dimension temperature distribution at the solid/fluid with different R_{alz}^* for: (a) FC-77 and (b) air.

The value of q'' could be found from modified Rayleigh number equation $R_{alz}^* = g\beta q'' L_z^4 / k_f \alpha_f \nu$ where the properties of FC-77 and air are constant and known and the cold wall has constant temperature at 20°C . So the temperature in dimension form could be found from the following:

$$T = \frac{\theta q'' L_z}{k_f} + T_c \tag{11}$$

Table II shows the values of heat flux q'' for both working fluids at two selected modified Rayleigh number 10^4 and 10^5 .

Table II. The values of q'' for different Modified Rayleigh Number for both working fluids.

R_{alz}^*	$q''(W/m^2)$ for FC-77	$q''(W/m^2)$ for air
10^4	52.1	240
10^5	521	2400

The results show that, there is a huge difference between the results of FC-77 and air. For example when $R_{alz}^* = 10^4$, the maximum temperature which is at heater one is 49.4°C and 23.3°C for air and FC-77 respectively, although the dimensionless temperature for air is less than that of FC-77. The same behaviour when $R_{alz}^* = 10^5$ where the maximum temperature of air is 5.5 times higher than that of the FC-77.

VI. DISCUSSION

Steady state natural conjugate convection analysis for rectangular cavity with discrete heat sources flush mounted on one vertical wall has been conducted numerically. The control volume technique with the "SIMPLE" algorithm was used to simulate the natural conjugate convection. The results from this research showed that:

1. The dimensionless temperature θ at solid/fluid interface for both working fluid (FC-77 and air) decreases as R_{alz}^* increase, that because the increment in the temperature differences is not equal to the increase in q'' .
2. For different working fluids the values of \hat{q}'' and local Nusselt number $Nu(X)$ increases when R_{alz}^* rises and that is due to the thermal boundary layer being thin and the local convection coefficient increased.
3. There was a strong effect of the substrate thermal conductivity on the temperature distribution as well as the maximum temperature. With increase R_s , more energy dissipated by substrate and that result a decrease of the maximum temperature level.
4. For high values of $R_s = 10^3$, the solid/fluid interface temperature considered isothermal where the discrete heater locations become almost indistinguishable. Moreover when the $R_s > 1500$ there is no anymore effect for the substrate on the maximum temperature.

REFERENCES

[1] A. Bar-Cohen, "Physical design of electronic systems--Methodology, technical trends, and future challenges. In: Advances in Thermal Modeling of Electronic Components and Systems," SME/IEEE Press, New York, vol. 3, pp. 1-60, 1993.

[2] A. E. Zinnes, "The coupling of conduction with laminar natural convection from a vertical fiat plate with arbitrary surface heating," *J. Heat Transfer*, vol. 92, pp. 528-535, 1970.

[3] M. Hasnaoui, E. Bilgen and P. Vasseur, "Natural convection heat transfer in rectangular cavities heated from below," *J. Thermophysical Heat Transfer*, vol. 6, pp. 255-264, 1992.

[4] A. Valencia and R. Frederick, "Heat Transfer in square cavities with partially active vertical walls," *Int. J. Heat and Mass Transfer*, vol. 32, pp. 1567-1574, 1989.

[5] E. Selamet, V. S. Arpaci and C. Borgnakke, "Simulation of laminar buoyancy driven flows in an enclosure," *Numerical Heat Transfer*, vol. 22, pp. 401-420, 1992.

[6] S. B. Sathe and Y. Joshi, "Natural convection arising from a heat generating substrate-mounted protrusion in a liquid-filled two-dimensional enclosure," *Int. J. Heat Mass Transfer*, vol. 34, pp. 2149-2163, 1991.

[7] Z. G. Du and E. Bilgen, "Coupling of wall conduction with natural convection in a rectangular enclosure," *Int. J. Heat Mass Transfer*, vol. 35, pp. 1969-1975, 1992.

[8] T. J. Heindel, S. Ramadhyani and F. P. Incropera, "Conjugate natural convection from an array of discrete heat sources: part 1 two- and three-dimensional model validation," *Int. J. Heat and Fluid Flow*, vol. 16, pp. 501-510, 1995.

[9] S. Banerjee, A. Mukhopadhyay, S. Sen and R. Ganguly, "Natural convection in a bi-heater configuration of passive electronic cooling," *Int. J. Thermal Sciences*, vol. 47, pp. 1516-1527, 2008.

[10] D. E. Wroblewski and Y. Joshi, "Computations of liquid immersion cooling for a protruding heat source in a cubical enclosure," *Int. J. Heat Mass Transfer*, vol. 36, pp. 1201-1218, 1993.

[11] D. E. Wroblewski and Y. Joshi, "Liquid immersion cooling of a substrate-mounted protrusion in a three-dimensional enclosure: The effects of geometry and boundary conditions," *J. Heat Transfer*, vol. 116, pp. 112-119, 1994.

[12] E. Bilgen, "Conjugate heat transfer by conduction and natural convection on a heated vertical wall," *Applied Thermal Engineering*, vol. 29, pp. 334-339, 2009.

[13] S. M. Aminossadati and B. Ghasemi, "Enhanced natural convection in an isosceles triangular enclosure filled with a nanofluid," *Computers and Mathematics with Applications*, vol. 61, no. 2, pp. 1739-1753, 2011.

[14] S. B. Sathe and Y. Joshi, "Natural convection liquid cooling of a substrate-mounted protrusion in a square enclosure: parametric study," *Int. J. Heat Transfer*, vol. 114, pp. 401-409, 1992.

[15] S. V. Patankar, "Numerical Heat Transfer and Fluid Flow," McGraw-Hill, (1980).

[16] T. J. Heindel, F. P. Incropera and S. Ramadhyani, "Conjugate natural convection from an array of discrete heat sources: part 2 -- a numerical parametric study," *Int. J. Heat and Fluid Flow*, vol. 16, pp. 511-518, 1995.